The Journal of Immunology

Neutrophil IL-1β Processing Induced by Pneumolysin Is Mediated by the NLRP3/ASC Inflammasome and Caspase-1 Activation and Is Dependent on K^+ Efflux

Mausita Karmakar, Michael Katsnelson, Hesham A. Malak, Neil G. Greene, Scott J. Howell, Amy G. Hise, Andrew Camilli, Aras Kadioglu, George R. Dubyak and Eric Pearlman

J Immunol 2015; 194:1763-1775; Prepublished online 21 January 2015;
doi: 10.4049/jimmunol.1401624
http://www.jimmunol.org/content/194/4/1763

The Journal of Immunology is published twice each month by
The American Association of Immunologists, Inc.,
1451 Rockville Pike, Suite 650, Rockville, MD 20852

Print ISSN: 0022-1767 Online ISSN: 1550-6606.

Neutrophil IL-1β Processing Induced by Pneumolysin Is Mediated by the NLRP3/ASC Inflammasome and Caspase-1 Activation and Is Dependent on K^+ Efflux

Mausita Karmakar,* Michael Katsnelson,† Hesham A. Malak,‡ Neil G. Greene,§ Scott J. Howell,* Amy G. Hise,¶ Andrew Camilli,§ Aras Kadioglu,‡ George R. Dubyak,† and Eric Pearlman*

Although neutrophils are the most abundant cells in acute infection and inflammation, relatively little attention has been paid to their role in inflammasome formation and IL-1β processing. In the present study, we investigated the mechanism by which neutrophils process IL-1β in response to *Streptococcus pneumoniae*. Using a murine model of *S. pneumoniae* corneal infection, we demonstrated a requirement for IL-1β in bacterial clearance, and we showed that Nod-like receptor protein 3 (NLRP3), apoptosis-associated speck-like protein containing a caspase activation and recruitment domain (ASC), and caspase-1 are essential for IL-1β production and bacterial killing in the cornea. Neutrophils in infected corneas had multiple specks with enzymatically active caspase-1 (YVAD-FLICA 660), and bone marrow neutrophils stimulated with heat-killed *S. pneumoniae* (signal 1) and pneumolysin (signal 2) exhibited multiple specks when stained for NLRP3, ASC, or Caspase-1. High–molecular mass ASC complexes were also detected, consistent with oligomer formation. Pneumolysin induced K^+ efflux in neutrophils, and blocking K^+ efflux inhibited caspase-1 activation and IL-1β processing; however, neutrophils did not undergo pyroptosis, indicating that K^+ efflux and IL-1β processing is not a consequence of cell death. There was also no role for lysosomal destabilization or neutrophil elastase in pneumolysin-mediated IL-1β processing in neutrophils. Taken together, these findings demonstrate an essential role for neutrophil-derived IL-1β in *S. pneumoniae* infection, and they elucidate the role of the NLRP3 inflammasome in cleavage and secretion of IL-1β in neutrophils. Given the ubiquitous presence of neutrophils in acute bacterial and fungal infections, these findings will have implications for other microbial diseases. ***The Journal of Immunology*****, 2015, 194: 1763–1775.**

Interleukin-1β plays an important role in infectious and in acute and chronic inflammatory diseases, including diabetes and ischemic injury (1, 2). Following activation of TLRs or other pathogen recognition molecules, IL-1β is translated as an inactive 34-kDa proform, which is subsequently cleaved to the active, 17-kDa form that can be secreted (3, 4). Although we and others have demonstrated a role for neutrophil proteases in cleavage (5–7), caspase-1 is the main enzyme that cleaves the IL-1β proform in macrophages and dendritic cells. Caspase-1 is also produced as an inactive proform that autocatalyzes its cleavage to the enzymatically active caspase-1, which occurs following oligomerization of inflammasome components, including the Nod-like receptor protein 3 (NLRP3) together with the adaptor molecule apoptosis-associated speck-like protein containing a caspase activation and recruitment domain (ASC) (3, 8).

In the present study, we demonstrate that neutrophils are the predominant source of IL-1β in a murine model of acute *Streptococcus pneumoniae* corneal infection, and that IL-1β cleavage is dependent on the NLRP3/ASC inflammasome and active caspase-1, which are detected multiple intracellular specks in neutrophils both in vitro and during infection. Furthermore, using highly purified human neutrophils, we show that secretion of mature IL-1β is induced by bacterial pneumolysin (Ply), and that the mechanism requires a rapid efflux of K^+ ions that precedes NLRP3 inflammasome activation and IL-1β cleavage without undergoing pyroptosis. Taken together, these findings elucidate a critical role for the NLRP3/ASC inflammasome and caspase-1 in IL-1β processing and secretion by neutrophils.

Materials and Methods

Sources of mice

C57BL/6 mice (6–10 wk old) were purchased from The Jackson Laboratory (Bar Harbor, ME), and IL-$1\beta^{-/-}$ mice were obtained from Dr. Y. Iwakura (University of Tokyo, Tokyo, Japan). Caspase-$1/11^{-/-}$ mice were generated by Richard Flavell (Yale University, New Haven, CT) as caspase-$1^{-/-}$ mice (9) and were subsequently found to be also deficient in caspase-11 (8, 10). $NLRP3^{-/-}$ and $ASC^{-/-}$ mice were generated by Millennium

*Department of Ophthalmology and Visual Sciences, Case Western Reserve University, Cleveland, OH 44106; †Department of Physiology and Biophysics, Case Western Reserve University, Cleveland, OH 44106; ‡Department of Clinical Infection, Microbiology and Immunology, Institute of Infection and Global Health, University of Liverpool, Liverpool L69 7BE, United Kingdom; §Graduate Program in Molecular Microbiology, Department of Molecular Biology and Microbiology and Howard Hughes Medical Institute, Sackler School of Graduate Biomedical Sciences, Tufts University School of Medicine, Boston, MA 02111; and ¶Department of Medicine, Louis Stokes Cleveland Veterans Affairs Medical Center, Cleveland, OH 44106

Received for publication June 26, 2014. Accepted for publication December 3, 2014.

This work was supported by National Institutes of Health Grants R01 EY14362 (to E.P.) and R01 GM36387 (to G.R.D.), Visual Sciences Research Center Core Grant P30 EY11373, as well as Cytometry and Imaging Microscopy Core Facility of the Comprehensive Cancer Center of Case Western Reserve University and University Hospitals of Cleveland Core Grant P30 CA43703. Additional support for this work was provided by the Research to Prevent Blindness Foundation and the Ohio Lions Eye Research Foundation. E.P. is the recipient of an Alcon Research Institute award, and A.C. is a Howard Hughes Medical Institute Investigator.

Address correspondence and reprint requests to Dr. Eric Pearlman, Department of Ophthalmology and Visual Sciences, Case Western Reserve University, 10900 Euclid Avenue, Cleveland, OH 44095. E-mail address: eric.pearlman@case.edu

The online version of this article contains supplemental material.

Abbreviations used in this article: ASC, apoptosis-associated speck-like protein containing a caspase activation and recruitment domain; cat, chloramphenicol acetyltransferase; hkSP, heat-killed *Streptococcus pneumoniae*; LDH, lactate dehydrogenase; NE, neutrophil elastase; NLRP3, Nod-like receptor protein 3; PdB, inactive pneumolysin toxoid; PFA, paraformaldehyde; Ply, pneumolysin; RT, room temperature; WT, wild-type.

Pharmaceuticals (Cambridge, MA). The NLRP3$^{-/-}$ mice were generated by homologous recombination in embryonic stem cells by replacing exons I and II of the cryopyrin gene (encoding the N-terminal pyrin domain) with an IRES/β-gal/neomycin resistance cassette, and therefore they are functional rather than complete knockout mice (11). Neutrophil elastase (NE)$^{-/-}$ mice were purchased from The Jackson Laboratory. All knockout mice were on a C57BL/6 background. Animals were housed in pathogen-free conditions in microisolator cages and were treated according to institutional guidelines after approval by the Case Western Reserve University Institutional Animal Care and Use Committee.

Bacterial strains and growth conditions

Wild-type (WT) encapsulated *S. pneumoniae* TIGR4 (serotype IV) was used in this study. To generate a Δ*ply* deletion mutant, the Ply coding region of TIGR4 was replaced with an antibiotic resistance cassette encoding chloramphenicol acetyltransferase (cat) via transformation of competent cells with a linear splicing by overlap extension PCR product. Approximately 1 kb flanking sequence on either side of Ply was amplified from TIGR4 genomic DNA using primer sets SP_1923 F1/SP_1923 R1 and SP_1923 F2/SP_1923 R2 (Supplemental Table I) for upstream and downstream sequences, respectively. The cat cassette was PCR amplified from pEVP3 using primer set Fcat/Rcat, and all three products were spliced together by overlap extension using primers SP_1923 F1 and SP_1923 R2. Competent TIGR4 bacteria were transformed with the resulting amplicon, and chloramphenicol-resistant colonies were selected on Fluka blood agar base no. 2 (Sigma-Aldrich) supplemented with 5% defibrinated whole sheep blood containing chloramphenicol (4 μg/ml). PCR and DNA sequencing were carried out to confirm replacement of Ply with the cat cassette. Both WT and Δply strains were routinely grown in Todd–Hewitt broth (Neogen) supplemented with 0.5% yeast extract in a 37°C and 5% CO_2 incubator. Bacteria were grown to mid-exponential phase such that there was 10^8 CFU/ml and diluted in sterile PBS to desired concentrations for corneal infection or in vitro stimulation. To generate heat-killed *S. pneumoniae* (hkSP), TIGR4 was diluted in sterile PBS and heated at 95°C for 5 min. Viability was confirmed by plating bacteria in a trypticase soy agar plate containing 5% defibrinated sheep blood (BD Biosciences).

Source of reagents

Recombinant Ply was expressed in *Escherichia coli* and purified as described (13, 14). Unless otherwise stated, the specific hemolytic activity of Ply was 100,000 hemolytic units/mg. The toxin was passed three times through an EndoTrap endotoxin removal column (Profos, Regensburg, Germany), after which LPS was undetectable using the PyroGene recombinant factor C assay (Lonza; detection limit 0.01 endotoxin units/ml). NF-κB inhibitor JSH23 (Sigma-Aldrich) and pJNK/AP-1 inhibitor SP600125 (Tocris Bioscience) were dissolved in DMSO and used at assay-dependent concentrations. Caspase-1 inhibitor YVAD (Bachem) and pan-caspase inhibitor ZVAD (ApexBio) were dissolved in DMSO and used at the indicated concentrations. Bafilomycin A (LC Laboratories), CA-074-Me (EMD Chemicals), and ZFA (Bachem) were dissolved according to the manufacturers' protocols. Nigericin (Calbiochem) was used at 10 μM concentration. High potassium medium for neutrophils had the following composition: 130 mM KCl, 1.5 mM $CaCl_2$, 1 mM $MgCl_2$, 25 mM HEPES, 5 mM glucose, and 0.1% BSA at pH 7.4. For low potassium medium, we added 5 mM KCl, keeping other components the same.

Murine model of S. pneumoniae *corneal infection*

Mice were anesthetized with 1.2% 2,2,2-tribromoethanol, and corneal epithelium of the mice was abraded using a 26-gauge needle through which a 2-μl injection containing ~10^5 TIGR4 in sterile PBS was released into the corneal stroma using a 33-gauge Hamilton syringe and mice were allowed to recover from anesthesia. Infected mice were anesthetized after 24 h and positioned in a three-point stereotactic mouse restrainer to monitor corneal opacification using a stereomicroscope and Spot RT Slider KE camera (Diagnostic Instruments). Images were uploaded into MetaMorph image analysis software (Molecular Devices) and percentage and total opacity were quantified as described (6, 12). For depletion of neutrophils, mice were injected with 250 μg NIMP-R14 Ab or IgG by i.p. injection 24 h prior to infection with ~10^5 TIGR4.

Quantification of streptococcal CFU

For assessment of bacterial viability, infected mice were euthanized by CO_2 asphyxiation and whole eyes were isolated and homogenized in 1 ml sterile PBS in Mixer Mill MM300 (Retsch) at 33 Hz for 3 min. Serial log dilutions of the bacteria were plated on blood agar plates, incubated in CO_2 incubator at 37°C for 18 h, and colony numbers were counted manually.

Flow cytometry of corneas and image stream analysis

Corneas from infected mice were excised using a surgical microscissor and incubated in type I collagenase (Sigma-Aldrich) at 82 U/cornea for 2 h at 37°C. The cell suspension was then passed through a 30-μm filter to remove any undigested tissue. Fc receptors were blocked for 20 min at room temperature (RT) with anti-mouse CD16/32 Ab (eBioscience) followed by incubation with Alexa Fluor 488-NIMP-R14 (in-house) and PE-F4/80 (eBioscience) Abs to detect neutrophils and macrophages, respectively. After staining, cells were washed in 2 ml FACS buffer (1% FBS in PBS) and fixed in 0.5% paraformaldehyde (PFA) for analysis by flow cytometry using an Accuri C6 flow cytometer (Becton Dickinson).

For intracellular cytokine staining, corneal cells were incubated at 4°C overnight with 1× Protein Transport Inhibitor Cocktail (eBioscience), fixed in 4% PFA, and permeabilized in 1× Perm buffer (eBioscience) for 10 min. Cells were then stained with allophycocyanin–pro-IL-1β Ab (eBioscience), washed in FACS buffer, and fixed in 0.5% PFA for analysis by flow cytometry or multispectral imaging flow cytometry (ImageStream 100; Amnis, Seattle, WA).

Amnis ImageStream^X and IDEAS analysis

Purified bone marrow neutrophils were primed for 3 h with hkSP (signal 1) and then stimulated with Ply (200 ng/ml). Unstimulated neutrophils were used as control. Following stimulation, the cells were stained with either FAM-YVAD-FMK (ImmunoChemistry Technologies) according to the manufacturer's protocol or with ASC mAb (clone 2EI-7; Millipore) followed by anti-mouse Alexa Fluor 488 secondary Ab. Acquisition was performed using an ImageStream^X imaging flow cytometer (Amnis) equipped with INSPIRE software as described (15). Briefly, a ×60 magnification was used to acquire images of all samples. A minimum of 10,000 cells were analyzed for each treated sample. FAM-YVAD-FMK–stained cells (for caspase-1) and ASC-stained cells were excited with a 100 mW 488-nm argon laser and were collected on channel two (505–560 nm). Intensity adjusted bright-field images were collected on channel one. Data analysis was performed using the IDEAS software (Amnis), and a compensation matrix was generated using singly stained samples. The compensated data were gated to eliminate cells that were not in the field of focus; second, the focused cells were gated to eliminate clumped cells and debris. The IDEAS software contains wizards to measure features, such as "count spots" associated with the cells. For the spot counting wizard, subpopulations of cells with no spots, low numbers of spots, and high numbers of spots were manually identified as truth sets, and the software used these datasets to determine the number of spots per cell.

Western blot analysis

Corneas were excised from the eyes using a microscissor. Any associated iris was removed, and clean corneas were homogenized in 1× cell lysis buffer (Cell Signaling Technology) supplemented with protease inhibitor mixture. For in vitro experiments, 4×10^6 cells were lysed in cell lysis buffer after appropriate stimulation. Twenty to thirty micrograms protein was fractionated in 12% SDS-PAGE, transferred into nitrocellulose membranes, and incubated with primary Abs, that is, mouse IL-1β (R&D Systems), mouse NLRP3 and ASC (AdipoGen International), human NLRP3 (Sigma-Aldrich), mouse caspase-1 p10 (Santa Cruz Biotechnology), mouse pJNK (T183/Y185) and total JNK (Cell Signaling Technology), and β-actin (Sigma-Aldrich). Reactivity was determined using HRP-conjugated secondary Abs (Santa Cruz Biotechnology) and developed with Super-Signal West Femto maximum sensitivity substrate (Pierce).

Isolation of human and mouse bone marrow neutrophils

Human neutrophils were isolated from the peripheral blood of healthy volunteers following informed consent as approved by the Institutional Review Board of University Hospitals of Cleveland. Heparinized blood was incubated with 3% dextran in PBS (Sigma-Aldrich) for 20 min at RT. The top clear layer containing leukocytes was transferred to a fresh tube and the cells were underlaid with 10 ml Ficoll-Paque Plus (GE Healthcare) and centrifuged at 300 × *g* for 20 min. The overlying plasma and PBMC layer were aspirated and the neutrophil/RBC pellets were suspended in 1× RBC lysis buffer (eBioscience). Cells were then washed in sterile PBS and resuspended in RPMI 1640 plus L-glutamine media (HyClone) supplemented with 2% FBS (Mediatech). Cell purity was determined for each experiment by Wright–Giemsa stain (Sigma-Aldrich) and routinely yielded >97% pure neutrophils.

For mouse bone marrow neutrophils, total bone marrow cells were collected from tibias and femurs. Neutrophils were isolated from the total bone marrow cells by negative selection using an EasySep mouse neutrophil enrichment kit (StemCell Technologies). After magnetic separation, cells were washed with PBS and resuspended in RPMI 1640 plus L-glutamine

with 2% FBS. This procedure routinely yielded >94% pure neutrophils as quantified by Wright–Giemsa stain.

Caspase-1 activation assay

Active caspase-1 was quantified by using a YVAD-FLICA 660 far red detection kit (ImmunoChemistry Technologies) according to the manufacturer's guidelines. Stained cells were either quantified by flow cytometry (using unstained cells to set the gate) or were visualized by confocal microscopy for active caspase-1 oligomerization.

Immunofluorescence staining

Stimulated human and mouse neutrophils were fixed with 4% PFA (Fisher Scientific) at RT for 15 min and permeabilized with 0.1% Triton X-100 for 10 min. Cells were then blocked in 10% goat or rabbit serum (Vector Laboratories) in PBS for 1 h at 22°C, followed by staining with a mAb to NLRP3 (clone EPR4777; Abcam) or ASC (Millipore) for 1 h at 37°C. Cells were then washed three times in PBS and counterstained with Texas red rabbit anti-goat IgG (Vector Laboratories) or Alexa Fluor 488 goat-anti mouse IgG (Invitrogen) for 40 min at RT. The cells were washed three times in PBS and stained with DAPI.

Confocal microscopy

Images were collected using an UltraVIEW VoX spinning disk confocal system (PerkinElmer) mounted on a Leica DMI6000B microscope equipped with an HCX PL APO ×100/1.4 oil immersion objectives using a 0.2-μm step size. Images were then imported into MetaMorph image analysis software (Molecular Devices) where maximum projections were generated from the original stacks and visualized following two-dimensional deconvolution.

ASC oligomerizarion assay

Stimulated murine neutrophils were lysed in RIPA lysis buffer (0.5% sodium deoxycholate, 0.1% SDS, and 1% Nonidet P-40) and centrifuged at 4000 × *g* for 10 min. Lysate was transferred to a fresh tube, and pellets were washed twice in 1× PBS and then cross-linked using dextran sulfate sodium (final concentration of 2 mM) for 30 min at RT. The cross-linked pellet was centrifuged at 4000 × *g* for 10 min, resuspended in Laemmli buffer, and fractionated in 12% SDS-PAGE. Western blot analysis was performed using anti-ASC Ab.

Atomic absorbance spectroscopy

After stimulation of mouse or human neutrophils, the extracellular medium was aspirated and the cells were rapidly washed in potassium-free isotonic buffer (135 mM sodium gluconate, 1.5 mM $CaCl_2$, 1 mM $MgCl_2$, and 25 mM HEPES). The washed cell pellets were then extracted into 1 ml 10% HNO_3. K^+ content in the nitric acid extracts was quantified by atomic absorbance spectrometry (Agilent 55B AA Spectrometer) as described previously (16). Triplicate samples were run for all test conditions in each experiment.

Detection of cytokines by ELISA

Half-well cytokine assays were performed using a DuoSet ELISA assay kit for IL-1β and CXCL8/IL-8 according to the manufacturer's protocols (R&D Systems).

Lactate dehydrogenase release assay

After stimulation of neutrophils, supernatant was collected and lactate dehydrogenase (LDH) release was quantified using a CytoTox 96 nonradioactive cytotoxicity assay (Promega) according to the manufacturer's instructions. Percentage cytotoxity was calculated based on LDH release in total cell lysate.

Statistical analysis

Student *t* test or ANOVA with Tukey post hoc analysis (Prism; GraphPad Software) were used as indicated in the figure legends. A p value ≤ 0.05 was considered significant.

Results

NLRP3, ASC, caspase-1, and IL-1β are required for protection against S. pneumoniae *corneal infection*

The normal avascular mammalian cornea has resident macrophages and dendritic cells, whereas neutrophils are only detected following an infectious or inflammatory event when they are recruited to the corneal stroma from peripheral, limbal vessels together with infiltrating macrophages and dendritic cells (17, 18). To examine the role of IL-1β on bacterial growth and corneal disease severity following corneal infection, *S. pneumoniae* (1×10^5 bacteria of strain TIGR4) was injected into the corneal stroma of C57BL/6 or IL-1β$^{-/-}$ mice. After 24 h, the total number of bacteria was assessed by CFU and infiltrating neutrophils and macrophages were quantified by flow cytometry using the NIMP-R14 Ab that recognizes Ly6G receptor, which we have shown reacts specifically with neutrophils (19), and the F4/80 Ab that primarily detects macrophages.

Quantification of infiltrating cells in the cornea showed significantly fewer neutrophils in infected IL-1β$^{-/-}$ compared with C57BL/6 corneas, whereas there was no significant difference in the number of infiltrating macrophages (Fig. 1A). Conversely, we found significantly higher CFU in IL-1β$^{-/-}$ corneas compared with C57BL/6 corneas (Fig. 1B). Representative bright-field images of *S. pneumoniae*–infected corneas show severe corneal opacity in C57BL/6 compared with IL-1β$^{-/-}$ mice (Fig. 1C), and quantification of corneal opacity revealed significantly higher corneal disease in C57BL/6 compared with IL-1β$^{-/-}$ mice (Fig. 1D, 1E). IL-1β$^{-/-}$ corneas perforate after 48 h owing to unrestricted bacterial growth (data not shown). H&E staining of corneal sections from infected eyes showed enhanced cellular infiltration in the corneal stroma of infected C57BL/6 compared with IL-1β$^{-/-}$ mice, which was comprised mostly of NIMP-R14$^+$ neutrophils (Supplemental Fig. 2).

Although we found no role for caspase-1 in *Pseudomonas aeruginosa* keratitis (6), we examined whether this protease was required for clearance of *S. pneumoniae*. Corneas of caspase-1/11$^{-/-}$ mice were therefore infected, and cellular infiltration, CFU, and corneal opacity were measured as before. As shown in Fig. 1F–J, caspase-1/11$^{-/-}$ mice had the same phenotype as IL-1β$^{-/-}$ mice, with significantly less neutrophil infiltration (Fig. 1F), impaired bacterial clearance (Fig. 1G), and less corneal opacification (Fig. 1H–J). Similar results were found for NLRP3$^{-/-}$ and ASC$^{-/-}$ mice compared with C57BL/6 mice (Fig. 1K–O).

Taken together, these data clearly implicate a role for IL-1β and the NLRP3/ASC inflammasome in regulating neutrophil infiltration and bacterial growth in *S. pneumoniae* corneal infection.

NLRP3 and ASC are required for caspase-1 activation and IL-1β processing by neutrophils during S. pneumoniae *corneal infection*

To assess whether the NLRP3/ASC inflammasome is required for IL-1β processing in vivo, corneas of C57BL/6, NLRP3$^{-/-}$, and ASC$^{-/-}$ mice were infected with *S. pneumoniae* as described above, and after 24 h corneas were homogenized and processed for Western blot analysis. Fig. 2A shows the p10 caspase-1 subunit and the processed p17 IL-1β bands in infected C57BL/6 corneas, but not in infected NLRP3$^{-/-}$ or ASC$^{-/-}$ corneas. Furthermore, ASC was present in the PBS-treated mice, whereas NLRP3 was detected only after *S. pneumoniae* infection.

To identify the cells producing intracellular pro–IL-1β, corneas of C57BL/6 mice were infected with *S. pneumoniae* as before, and after 24 h corneas were digested with collagenase and cells were stained with NIMP-R14, F4/80, and intracellular IL-1β and examined by flow cytometry. We found a distinct population of neutrophils in infected corneas expressing intracellular pro–IL-1β, comprising >20% of the total corneal cells (Fig. 2B). Furthermore, 85% of total pro–IL-1β-producing cells in the cornea were NIMP-R14$^+$ neutrophils compared with F4/80$^+$ macrophages, which accounted for <15% of the total IL-1β$^+$ cells (Fig. 2B).

To determine whether neutrophils are producing active caspase-1, *S. pneumoniae*–infected C57BL/6 corneas were digested with collagenase, and total corneal cells were stained with NIMP-R14 and FLICA 660–YVAD, a fluorescent peptide that binds to active

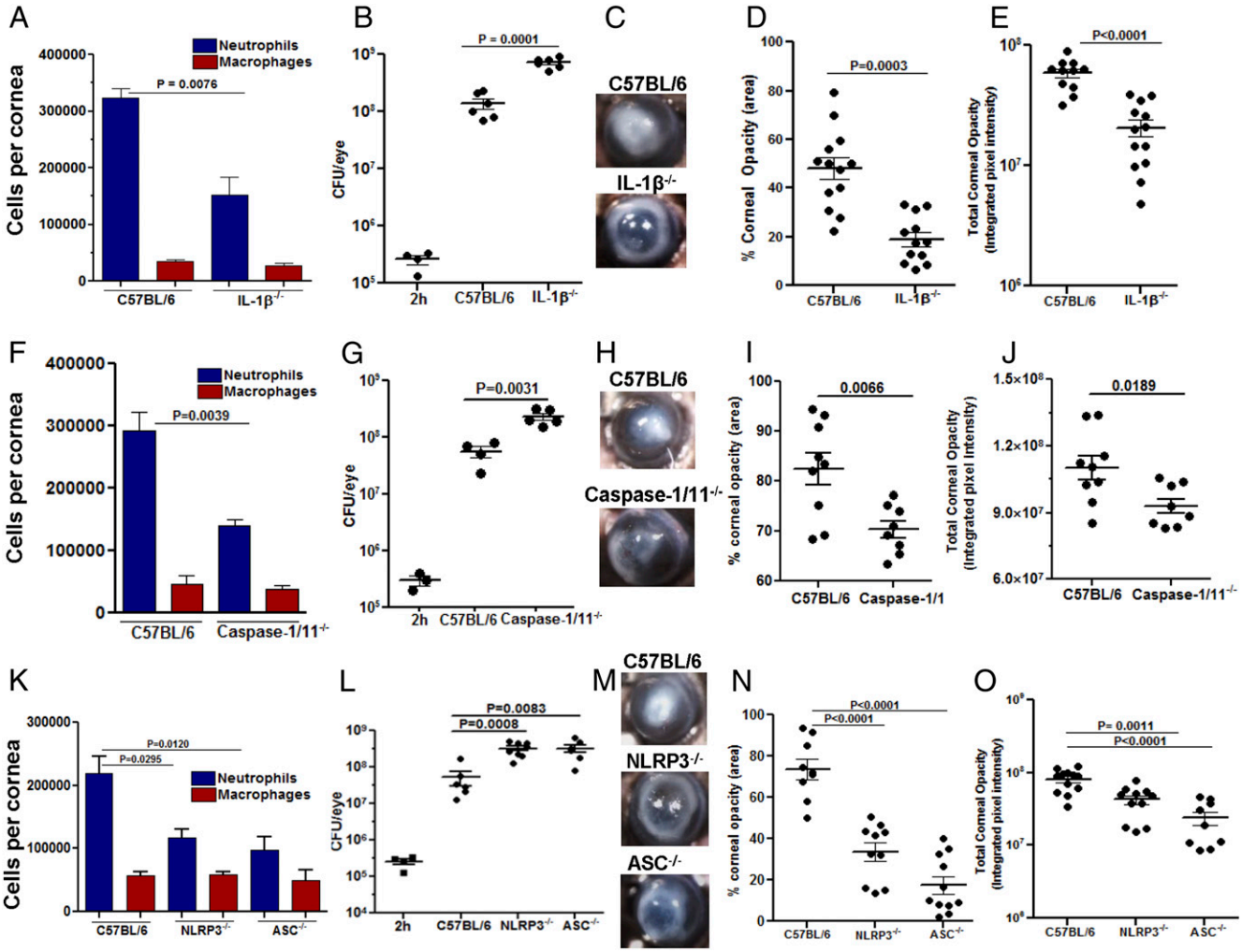

FIGURE 1. The role of IL-1β, NLRP3, ASC, and caspase-1 in *S. pneumoniae* keratitis. C57BL/6, IL-1β$^{-/-}$, caspase-1/11$^{-/-}$ NLRP3$^{-/-}$, and ASC$^{-/-}$ mice were infected in the corneal stroma with *S. pneumoniae* TIGR4. (**A**, **F**, and **K**) Total NIMP-R14^{+} neutrophils and F4/80^{+} macrophages in infected corneas were quantified by flow cytometry. (**B**, **G**, and **L**) Total CFU in eyes of infected mice after 2 h (inoculum) and after 24 h. (**C**, **H**, and **M**) Representative bright-field images of corneas 24 h postinfection. Original magnification ×30. (**D**, **I**, and **N**) Percentage and (**E**, **J**, and **O**) total corneal opacification calculated by MetaMorph analysis as shown in Supplemental Fig. 1. (A, F, and K) Mean ± SD of five samples per group. For CFU and corneal opacification graphs, each datum point represents a single cornea. Results are representative of three independent experiments with at least five mice per group.

caspase-1 and that has been used to detect active caspase-1 in macrophages (20, 21). We found that >30% of total cells in the cornea were FLICA 660–YVAD^{+} neutrophils, and >75% caspase-1^{+} cells in the cornea were NIMP-R14^{+} neutrophils (Fig. 2C). Active caspase-1 in neutrophils was also detected as speck-like aggregates as shown by multispectral imaging flow cytometry (Fig. 2D).

To examine the role of neutrophils in IL-1β processing and NLRP3 expression, neutrophils were depleted in C57BL/6 mice by i.p. injection of NIMP-R14 24 h before infection with *S. pneumoniae*. Systemic neutrophil depletion was confirmed by flow cytometry (Supplemental Fig. 3), and corneas from *S. pneumoniae*–infected mice were examined for NLRP3 and IL-1β production. As shown in Fig. 2E, there was decreased expression of NLRP3 and pro–IL-1β in neutrophil-depleted mice, and no mature IL-1β was detected. Additionally, there was decreased corneal opacity (Fig. 2F) and significantly increased CFU in neutrophil-depleted mice (Fig. 2G). These findings support the concept that neutrophils are essential for production of mature IL-1β and for bacterial killing. Although we cannot eliminate the possibility of a role for macrophages, our findings indicate that neutrophils are the major source of IL-1β in *S. pneumoniae* corneal infection.

NLRP3/ASC expression and oligomerization in murine bone marrow neutrophils

To examine the expression of NLRP3 and ASC, bone marrow neutrophils from C57BL/6 and NLRP3$^{-/-}$ mice were incubated for 3 h with hkSP (signal 1), and proteins were detected by Western blot. NLRP3 expression was low in unstimulated neutrophils, but was induced over time after stimulation with hkSP as signal 1 (Fig. 3A). In contrast, ASC was constitutively expressed in unstimulated C57BL/6 and NLRP3$^{-/-}$ neutrophils (Fig. 3A).

Because TLR2 is elevated in corneas of individuals with *S. pneumoniae* corneal ulcers, and TLR2 modulates the severity of murine *S. pneumoniae* corneal infection (22, 23), we examined the role of TLR2 in NLRP3 and ASC expression. Bone marrow neutrophils from C57BL/6 and TLR2$^{-/-}$ mice were stimulated 3 h with hkSP, and expression of NLRP3 and ASC was detected by Western blot analysis. Fig. 3B shows decreased NLRP3 expression in TLR2$^{-/-}$ compared with C57BL/6 neutrophils, whereas expression of ASC remained unchanged. To examine other mediators of TLR2 signaling on NLRP3 expression, C57BL/6 neutrophils were incubated with the NF-κB inhibitor JSH-23 or the JNK inhibitor SP600125. We found that NLRP3 expression

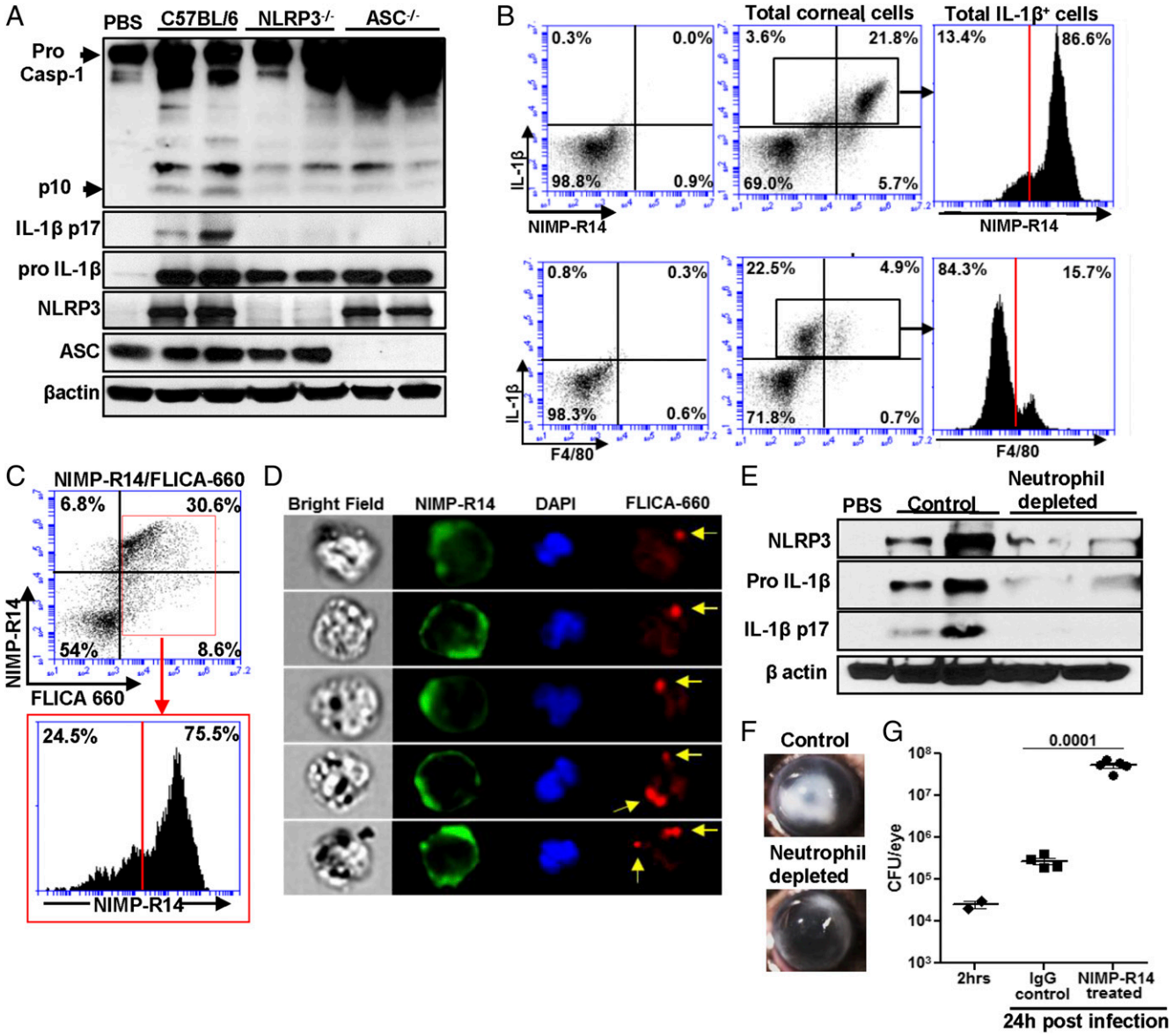

FIGURE 2. NLRP3 and ASC are required for caspase-1 activation and IL-1β processing by neutrophils during *S. pneumoniae* corneal infection. C57BL/6, NLRP3$^{-/-}$, and ASC$^{-/-}$ mice were infected in the corneal stroma with *S. pneumoniae* TIGR4. (**A**) Twenty-four hours after infection, corneas were excised and homogenized in lysis buffer and Western blot was performed for mature forms of caspase-1 (p10) and IL-1β (p17), which are indicated by arrowheads. (**B**) Flow cytometric analysis (*left panels*) of intracellular pro–IL-1β in neutrophils and macrophages from infected C57BL/6 corneas after 24 h. Gates were determined based on an isotype control. (**C**–**E**) C57BL/6 mice were infected with *S. pneumoniae*, and 24 h later corneas were excised and digested in collagenase. Total corneal cells were incubated with NIMP-R14 and FLICA 660–YVAD to detect active caspase-1–producing neutrophils by flow cytometry (C). NIMP-R14 (green) and FLICA 660–YVAD (red) cells were detected by multispectral imaging flow cytometry (D). Original magnification ×60. (E–**G**) Neutrophils were depleted in C57BL/6 mice by i.p injection of NIMP-R14 Ab 24 h prior to infection with *S. pneumoniae* TIGR4. Twenty-four hours after infection, corneas were excised and homogenized in lysis buffer and Western blot was performed for NLRP3, pro–IL-1β, and mature IL-1β (E). Representative bright-field images show corneal opacification (F). Original magnification ×20. (G) CFU in infected eyes was quantified 24 h postinfection. Data points represent individual eyes. These experiments were repeated twice with similar results.

was completely inhibited in the presence of JSH-23 and partially inhibited by SP600125 (Fig. 3C, 3D), although there was no effect of either inhibitor on ASC expression.

Taken together, these data indicate that *S. pneumoniae* induces NLRP3 expression by TLR2 activation through the NF-κB pathway and to some extent the MAPK/AP-1 pathway, whereas ASC expression in neutrophils is constitutive.

The active NLRP3 inflammasome forms large, multimeric complexes with ASC in macrophages and dendritic cells (3, 24). To investigate NLRP3 and ASC oligomerization in neutrophils, bone marrow neutrophils from C57BL/6 mice were incubated 3 h with hkSP (signal 1), followed by 2 h stimulation with live WT TIGR4, recombinant hemolytic Ply, or with the inactive Ply toxoid (PdB) as signal 2, and intracellular NLRP3 was detected by confocal microscopy using the same mAb to NLRP3 (clone Nalpy3b; Abcam) used by others (25, 26). NLRP3 expression was very low in unstimulated neutrophils; however, following incubation with hkSP, there was enhanced NLRP3 expression in the cytosol (Fig. 3E). This is also consistent with our observation in Fig. 3A that priming with hkSP induces NLRP3 expression in murine and human neutrophils. However, after further incubation with live TIGR4 or active Ply, NLRP3 was detected as speck-like aggregates in neutrophils. Furthermore, specks were not detected in neutrophils incubated with nonhemolytic PdB. This diffuse

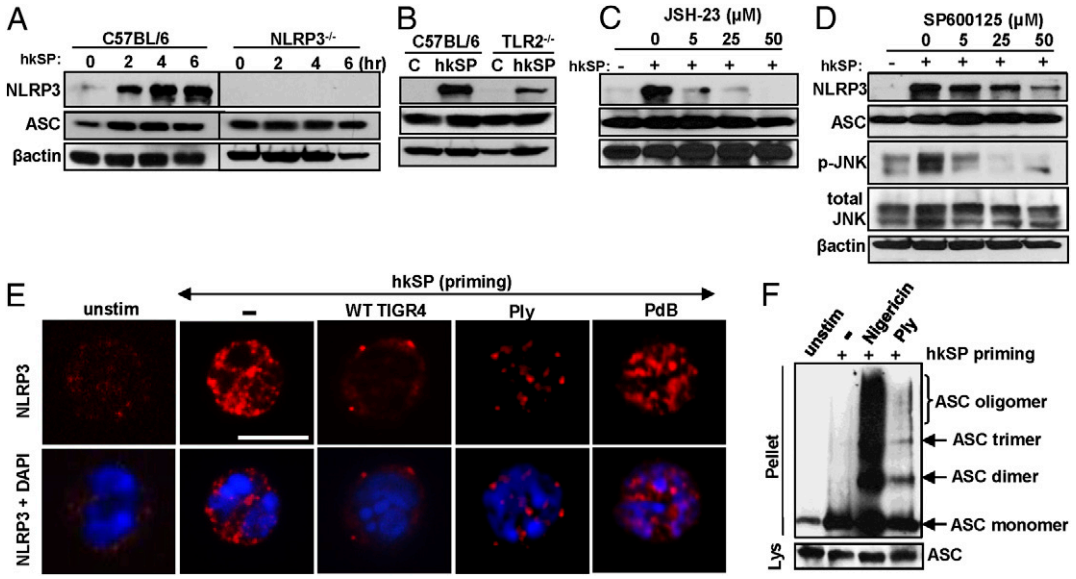

FIGURE 3. NLRP3/ASC expression and oligomerization in neutrophils. (**A**) NLRP3 protein expression by Western blot of C57BL/6 bone marrow neutrophils after incubation with hkSP for 3 h. (**B**) NLRP3 protein expression in bone marrow neutrophils from C57BL/6 and TLR2$^{-/-}$ mice after stimulation with hkSP for 3 h. (**C** and **D**) NLRP3 expression in C57BL/6 neutrophils incubated with either NF-κB inhibitor JSH-23 (C) or the JNK/AP-1 inhibitor SP600125 (D) at the indicated concentrations (μM) for 30 min prior to stimulation with hkSP for 3 h. Western blot was performed for NLRP3, ASC, p-JNK, total JNK, and β-actin. (**E**) NLRP3 expression in C57BL/6 bone marrow neutrophils after priming with hkSP for 3 h followed by stimulation with WT TIGR4 (multiplicity of infection of 50), Ply, or a nonhemolytic Ply (PdB) for 1.5 h. Red is NLRP3 and blue is DAPI. Scale bar, 10 μm. (**F**) ASC oligomers detected by Western blot from C57BL/6 bone marrow neutrophils after priming with hkSP for 3 h followed by stimulation with Ply (500 ng/ml) for 2 h or with nigericin (10 μM) for 45 min. Western blot was performed from the pellet and lysate (Lys) using anti-ASC Ab. Data are representative of two repeat experiments.

staining with signal 1 and the presence of multiple NLRP3$^+$ specks throughout the neutrophils following signal 2 are also clearly detected in Supplemental Videos 1 and 2. To detect ASC oligomerization, neutrophils were stimulated with Ply or nigericin, and lysates were cross-linked using dextran sulfate sodium and examined by Western blot analysis using an mAb to ASC. As shown in Fig. 3F, ASC was detected as monomers in unstimulated cells, but as multimers in Ply- and nigericin-stimulated neutrophils.

These findings demonstrate that not only do neutrophils express NLRP3 and ASC, but they also form multiple large multimeric complexes more typically seen in macrophages and dendritic cells.

Ply-stimulated neutrophils have multiple caspase-1 and ASC specks

To quantify the number of caspase-1 and ASC specks in neutrophils, bone marrow neutrophils from C57BL/6 mice were primed for 3 h with hkSP followed by 2 h stimulation with purified Ply. Cells were then stained with Ab to ASC or with FAM-YVAD-FMK and analyzed by Amnis ImageStream, and the number of specks associated with each cell was quantified using IDEAS software. Representative neutrophils analyzed are shown as bright-field images (channel 1) and green fluorescent specks (channel 2) expressing one or multiple ASC specks (Fig. 4A, 4D). Most of the neutrophils (56.2%) expressed two or more ASC specks, and the actual numbers and percentages are shown in Fig. 4B and 4C.

Representative neutrophils stained with FAM-YVAD-FMK for caspase-1 activity are shown in Fig. 4D, and quantification shows very similar numbers as ASC specks, with 66.4% neutrophils having two or more specks (Fig. 4E, 4F). The specificity of FAM-YVAD-FMK stain was confirmed using caspase-1/11$^{-/-}$ neutrophils, which showed significantly reduced number of caspase-1 specks compared with C57BL/6 neutrophils after stimulation with Ply (Supplemental Fig. 3). The presence of caspase-1$^+$ cells and specks in caspase 1/11$^{-/-}$ mice is likely due to cross-reactivity of FAM-YVAD-FMK with other proapoptotic caspases that are expressed in neutrophils.

Taken together, these data indicate that in contrast to macrophages and dendritic cells, murine bone marrow neutrophils express multiple caspase-1 and ASC specks following activation of NLRP3 inflammasome by Ply.

Caspase-1 activation in neutrophils is dependent on NLRP3 and ASC and requires active Ply

To determine whether live *S. pneumoniae* can activate caspase-1 in neutrophils, murine bone marrow neutrophils from C57BL/6 mice were incubated 3 h with hkSP (signal 1), followed by 2 h stimulation with live TIGR4 *S. pneumoniae* or with an isogenic mutant deleted for the gene encoding Ply (Δ*ply*) (signal 2), and active caspase-1 was quantified using FLICA 660–YVAD.

Caspase-1 staining was detected as speck-like structures in neutrophils following incubation with *S. pneumoniae* TIGR4 strain expressing Ply, but not with the Δ*ply* mutant or with hkSP alone (Fig. 5A). Consistently, there was a significantly higher percentage of FLICA 660–YVAD$^+$ neutrophils after incubation with live *S. pneumoniae* compared with neutrophils stimulated with the Δ*ply* mutants or hkSP alone (Fig. 5B).

To determine whether recombinant Ply can induce caspase-1 activation in neutrophils, bone marrow neutrophils from C57BL/6 mice were primed with hkSP as before and incubated with either a highly purified Ply that has pore-forming activity or with a mutant Ply (PdB) that has a single amino acid substitution resulting in diminished hemolytic activity (14). The percentage FLICA 660–YVAD$^+$ neutrophils was assessed by flow cytometry. Fig. 5C shows a distinct population of FLICA 660–YVAD$^+$ neutrophils following stimulation with hemolytic Ply (*left panel*) but not with PdB (*right panel*). Quantification of FLICA 660–YVAD$^+$ cells showed >80% caspase-1 expressing neutrophils in the presence of Ply compared with <10% in PdB-treated cells (Fig. 5D).

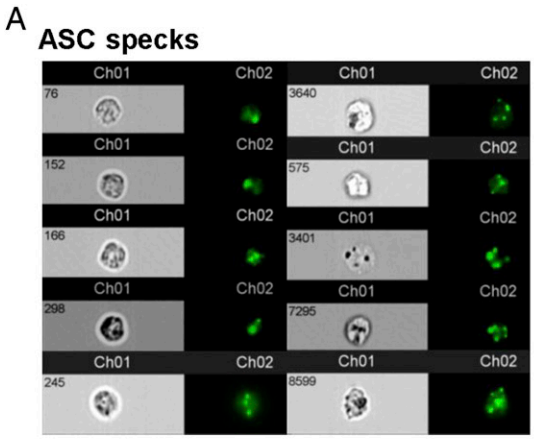

B

	No. of cells	% cells
Total cells with ASC specks	6547	100
Cells with 1 speck	2867	43.8
2 specks	1936	29.6
3 specks	1050	16
4 specks	428	6.54
5 specks	162	2.47
more than 6 specks	95	1.45

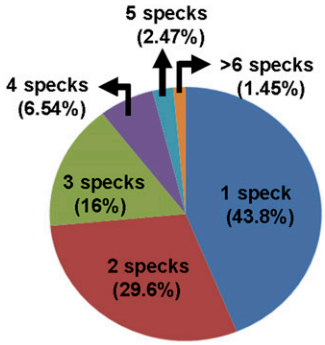

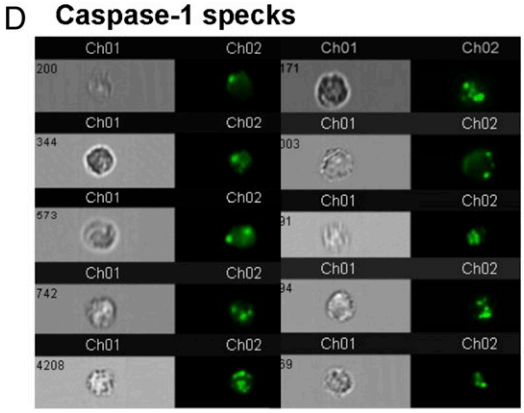

E

	No. of cells	% cells
Total cells with caspase-1 specks	3055	100
Cells with 1 speck	1019	33.4
2 specks	884	28.9
3 specks	581	19
4 specks	343	11.2
5 specks	133	4.35
more than 6 specks	88	2.88

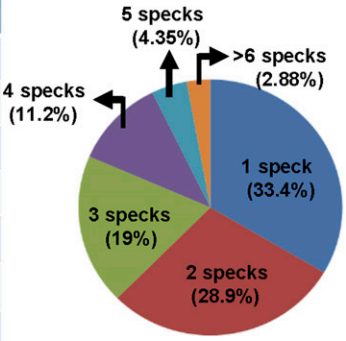

FIGURE 4. Multiple caspase-1 and ASC specks in neutrophils. Bone marrow neutrophils were isolated from C57BL/6 mice and primed for 2 h with hkSP and stimulated with purified Ply for 2 h. Cells were then stained with Ab to ASC or with FAM-YVAD-FMK (for caspase-1). (**A**) Representative bright-field and fluorescent images (original magnification ×60) of neutrophils showing ASC specks. (**B** and **C**) Neutrophils ($n = 6547$) were analyzed by Amnis ImageStream^X and spot counting was performed using IDEAS software; tables and pie charts were generated showing percentage and total number of neutrophils with one or multiple ASC specks. (**D**) Representative bright-field and fluorescent images (original magnification ×60) of neutrophils showing caspase-1 speck (FAM-YVAD-FMK staining). (**E** and **F**) Percentage and total number of neutrophils with one or multiple caspase-1 specks (3055 cells were analyzed). Ch, channel.

To assess the role of the NLRP3 inflammasome in Ply-induced caspase-1 and IL-1β processing, NLRP3$^{-/-}$, ASC$^{-/-}$, and caspase-1/11$^{-/-}$ neutrophils were primed with hkSP and stimulated with Ply as before, and the cleaved p10 form of caspase-1 in cell supernatants was TCA precipitated and detected by Western blot analysis. Caspase-1 p10 was clearly detected in supernatants from stimulated compared with unstimulated C57BL/6 neutrophils; however, caspase-1 p10 expression was markedly less in NLRP3$^{-/-}$, ASC$^{-/-}$, and caspase-1/11$^{-/-}$ neutrophils compared with C57BL/6 neutrophils (Fig. 5E). Similarly, there were significantly fewer FLICA 660–YVAD$^+$ cells in caspase-1/11$^{-/-}$, NLRP3$^{-/-}$, and ASC$^{-/-}$ compared with C57BL/6 neutrophils (Fig. 5F, 5G) and less secreted IL-1β following stimulation with live *S. pneumoniae* or purified Ply (Fig. 5H).

Taken together, these data indicate that *S. pneumoniae* pore-forming toxin Ply induces NLRP3/ASC-dependent caspase-1 activation and IL-1β secretion by neutrophils.

Ply mediates IL-1β processing and secretion from human neutrophils

To ascertain whether *S. pneumoniae*–mediated activation of the NLRP3 inflammasome in human neutrophils is dependent on the hemolytic activity of Ply, we stimulated human neutrophils with a Ply deletion mutant (Δ*ply*) or highly purified preparations of active hemolytic Ply and the nonhemolytic toxoid (PdB). Human peripheral blood neutrophils were primed with hkSP for 3 h to induce expression of pro–IL-1β and NLRP3 and were then stimulated with live WT TIGR4 or with mutant Δ*ply*.

IL-1β production by neutrophils was increased following incubation with increasing numbers of *S. pneumoniae* TIGR4; however, IL-1β was significantly reduced when neutrophils were stimulated with the TIGR4 Δ*ply* mutant (Fig. 6A). Similarly, neutrophils incubated with purified Ply produced IL-1β in a dose-dependent fashion, whereas the nonhemolytic Ply (PdB) induced significantly less IL-1β (Fig. 6B). In contrast to IL-1β, neutrophil-derived CXCL8 (IL-8) production was not significantly different when neutrophils were stimulated with the Δ*ply* mutant or the TIGR4 parent strain (Fig. 6C); there was also no difference in CXCL8 in neutrophils stimulated with PdB compared with Ply (Fig. 6D), indicating that the role of active Ply on IL-1β release from human neutrophils is not a general phenomenon. Neutrophils incubated with either live *S. pneumoniae* or purified Ply did not release LDH (Fig. 6E, 6F), indicating that IL-1β secretion by neutrophils occurs independently of pyroptosis.

These findings demonstrate that *S. pneumoniae*–induced IL-1β secretion from human neutrophils is dependent on the hemolytic activity of Ply and is not a result of cell lysis.

Ply-induced caspase-1 activation and IL-1β secretion by neutrophils requires K^+ efflux

Because activation of NLRP3 inflammasome in macrophages and dendritic cells can occur following a loss of cytosolic K^+ (27), we

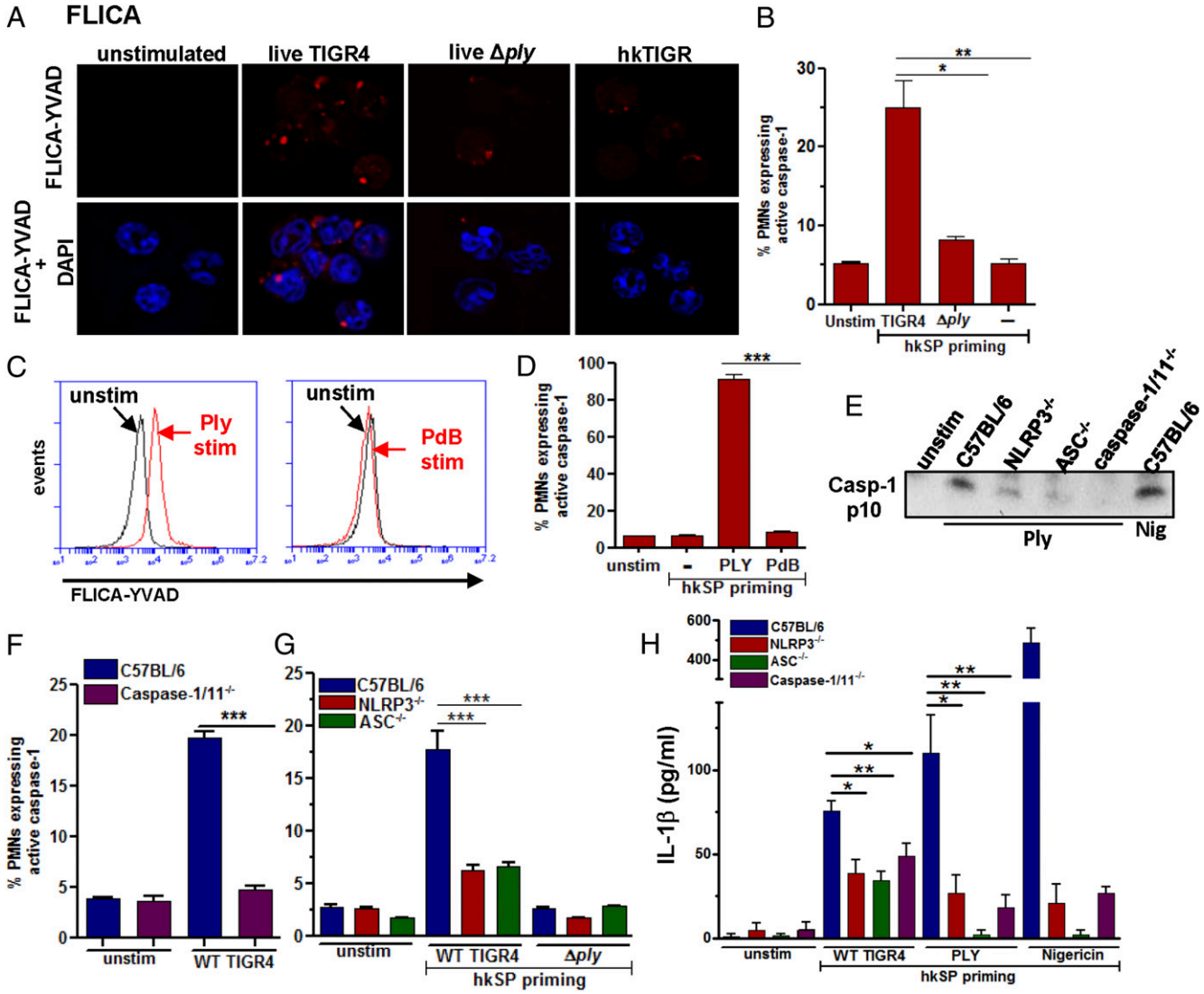

FIGURE 5. Active caspase-1 induction in murine neutrophils is dependent on NLRP3 and ASC and requires active Ply. C57BL/6 neutrophils were incubated 3 h with hkSP (signal 1), followed by 1.5 h stimulation with either live *S. pneumoniae* TIGR4 (WT) or the Δ*ply* mutant (signal 2), and active caspase-1 was detected using FLICA 660–YVAD. (**A**) Representative neutrophils showing FLICA 660–YVAD$^+$ cells (red specks) (original magnification ×100). (**B**) Percentage FLICA 660–YVAD$^+$ neutrophils. (**C** and **D**) Representative flow cytometry profiles (C) and percentage (D) FLICA 660–YVAD$^+$ C57BL/6 neutrophils primed with hkSP and further incubated with Ply or the nonhemolytic Ply (PdB) for 1.5 h. (**E**) Mature p10 form of caspase-1 from supernatant of C57BL/6, NLRP3$^{-/-}$, ASC$^{-/-}$, and caspase-1/11$^{-/-}$ neutrophils after incubation with Ply (500 ng/ml) for 2 h or with nigericin as a positive control. (**F** and **G**) Percentage FLICA 660–YVAD$^+$ neutrophils from C57BL/6 and caspase-1/11$^{-/-}$ mice (F) and from NLRP3$^{-/-}$ and ASC$^{-/-}$ mice (G) following hkSP priming for 3 h and stimulation with live WT or Δ*ply* mutants for 1.5 h. (**H**) IL-1β secretion after hkSP priming and stimulation with WT TIGR4 and purified Ply (500 ng/ml) for 2 h or nigericin for 45 min. Data are representative of three repeat experiments. $*p < 0.05$, $**p < 0.001$, $***p < 0.0001$.

examined the effect of Ply in mediating K^+ efflux from neutrophils.

Primed human peripheral blood neutrophils were incubated for 2 h with hemolytic (Ply) or nonhemolytic Ply (PdB), and total intracellular K^+ in cell lysates was measured by atomic absorbance spectrometry. Fig. 7A shows a dose-dependent decrease in cell-associated K^+ following incubation with Ply, consistent with enhanced K^+ efflux. Intracellular K^+ was significantly lower in neutrophils incubated with PdB, thereby indicating an essential role in pore-forming activity of Ply in inducing K^+ efflux from neutrophils. Conversely, when neutrophils were incubated in high extracellular K^+, which prevents formation of a plasma membrane K^+ gradient, the Ply-induced caspase-1 activation and IL-1β secretion were completely ablated (Fig. 7B, 7C), indicating that K^+ efflux is critical for caspase-1 activation and IL-1β secretion by Ply-stimulated neutrophils.

In addition to cleaving pro–IL-1β, caspase-1 also mediates pyroptotic cell death, which is characterized by loss of plasma membrane integrity and release of cytoplasmic contents, including LDH (28, 29). We therefore examined whether Ply-induced K^+ efflux occurs as a secondary consequence of pyroptotic cell death, that is, after caspase-1 activation, or whether K^+ efflux is an early signal for NLRP3 inflammasome assembly and IL-1β secretion, that is, before caspase-1 activation. Human neutrophils were primed with hkSP and incubated with Ply or nigericin in the presence of the caspase-1 inhibitor YVAD or the pan-caspase inhibitor ZVAD, and IL-1β secretion, intracellular K^+, and LDH release were measured.

As shown in Fig. 7D, IL-1β secretion by neutrophils stimulated with Ply or nigericin was completely inhibited in the presence of YVAD or ZVAD, indicating a requirement for caspase-1 in Ply-induced IL-1β secretion. In contrast, Ply-induced K^+ efflux (loss

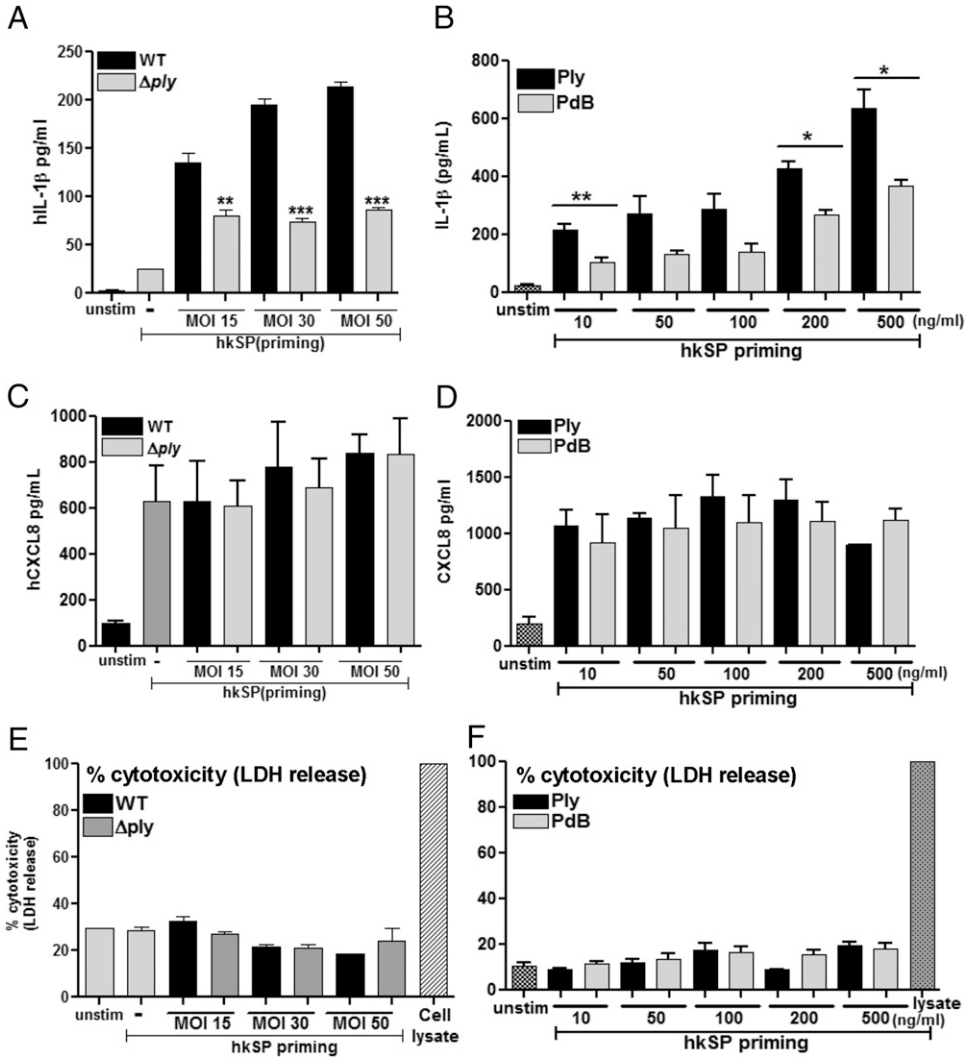

FIGURE 6. Ply-dependent caspase-1 activation and IL-1β secretion by human neutrophils. Human peripheral blood neutrophils were primed with hkSP for 3 h followed by 2 h stimulation with WT or Δ*ply* mutant *S. pneumoniae* (**A**, **C**, and **E**) or with Ply or PdB for 2 h (**B**, **D**, and **F**), and IL-1β (A and B) and CXCL8 (C and D) in the supernatant were quantified by ELISA. Cell death was assayed by LDH release compared with lysed cells (E and F). Histograms are means ± SD of at least five samples per group, and data shown are representative of three independent experiments. Nigericin (Nig) incubation was for 45 min. $*p < 0.05$, $**p < 0.005$, $***p < 0.0005$.

of intracellular K^+) was not inhibited by caspase-1 inhibitors (Fig. 7E), indicating that K^+ efflux occurs upstream of caspase-1 activation. Similarly, Ply-induced LDH release in the presence of caspase-1 inhibitors was not significantly different from Ply alone, indicating that neutrophils are not undergoing caspase-1–dependent pyroptosis (Fig. 7F).

Therefore, the results of these studies support the concept that Ply induces IL-1β secretion in neutrophils by causing loss of intracellular K^+ and activation of the NLRP3 inflammasome and that K^+ efflux is an early signal for inflammasome activation in neutrophils.

Ply-induced IL-1β secretion by neutrophils does not require lysosomal disruption or serine proteases activity

Activation of the NLRP3 inflammasome in monocytes and dendritic cells can be induced by lysosomal destabilization and cathepsin B release (14, 30, 31). Additionally, because serine proteases such as neutrophil elastase can also cleave pro–IL-1β to the mature form (6, 32–34), we investigated the role of lysosomal disruption and serine proteases in Ply-mediated IL-1β secretion by neutrophils.

To examine the role of cathepsin B on inflammasome activation and IL-1β release, neutrophils were incubated with purified Ply or *S. pneumoniae* TIGR4 in the presence of cathepsin B inhibitors CA-074-Me, ZFA, or with bafilomycin A, which blocks lysosomal acidification by inhibiting H^+-ATPase. Fig. 8A shows that IL-1β secretion by Ply or *S. pneumoniae* TIGR4–stimulated neutrophils in the presence of cathepsin B inhibitors or with bafilomycin A was not significantly different from cells in the absence of inhibitors, indicating that neither cathepsin B nor lysosomal destabilization is required for Ply-induced IL-1β processing in neutrophils. LDH release was not increased following incubation with these inhibitors, indicating that they are not cytotoxic at the concentrations used (Fig. 8B).

Additionally, we found no difference in IL-1β secretion or LDH release by *S. pneumoniae*–stimulated bone marrow neutrophils from $NE^{-/-}$ mice compared with C57BL/6 neutrophils (Fig. 8C, 8D), indicating that there is no role for elastase in IL-1β processing, and also that Ply-induced IL-1β processing by neutrophils does not require serine protease or cathepsin B activity.

Discussion

S. pneumoniae is the causative organism of pneumococcal septicemia, meningitis, and pneumonia, which result in infant mortality

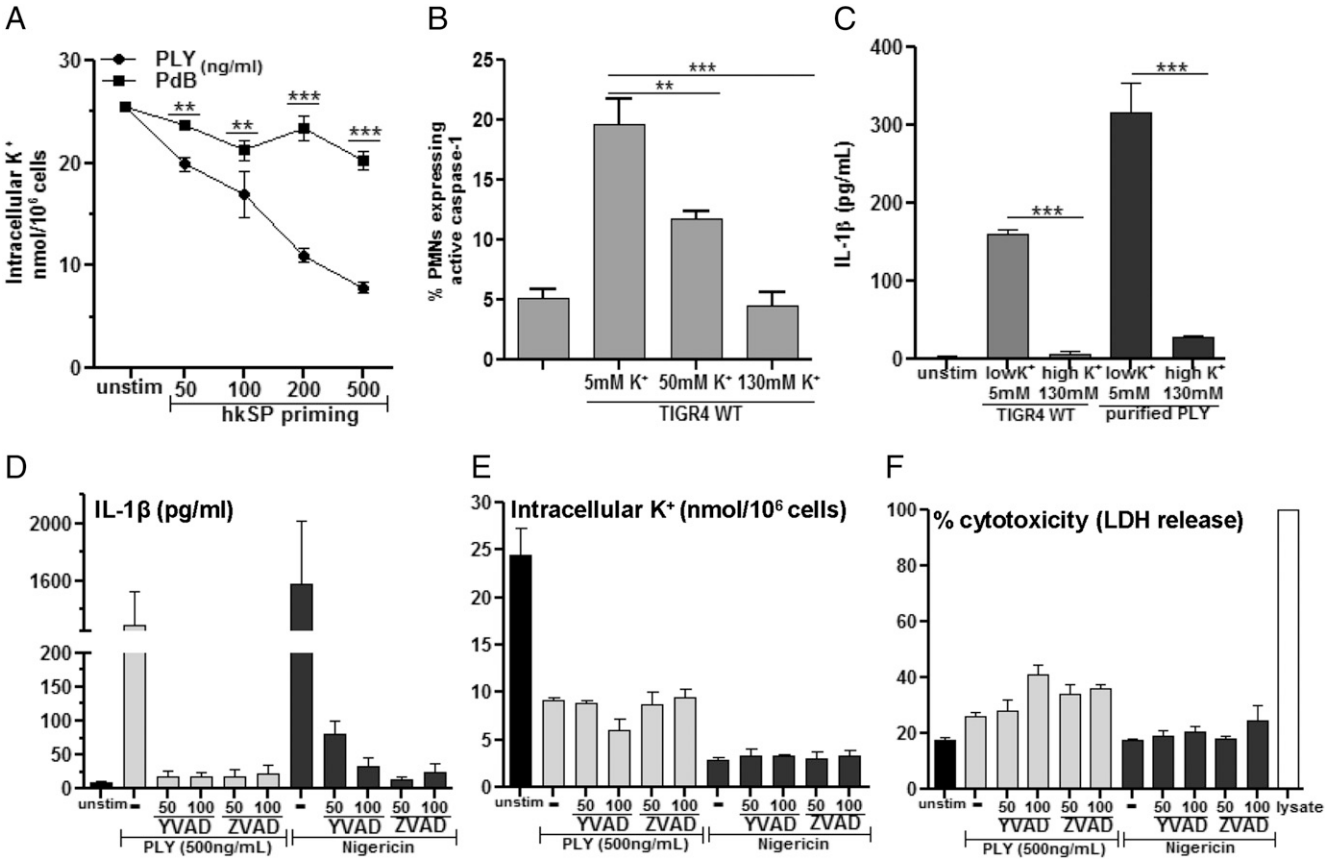

FIGURE 7. Ply-induced caspase-1 activation and IL-1β secretion by neutrophils requires K^+ efflux. (**A**) Human peripheral blood neutrophils were primed with hkSP for 3 h and stimulated with Ply or PdB for 2 h. Total cell contents were extracted using 10% HNO_3, and the cell-associated K^+ concentration was quantified by atomic absorbance spectroscopy. (**B**) FLICA 660–YVAD$^+$ murine neutrophils quantified by flow cytometry after treatment with live TIGR4 in the presence of increasing concentration of extracellular KCl. (**C**) hkSP-primed neutrophils were stimulated 2 h with either Ply (500 ng/ml) or WT TIGR4 (50:1) in either 5 or 130 mM KCl, and IL-1β secretion was measured. (**D**–**F**) Neutrophils were primed and stimulated with Ply (500 ng/ml) or were stimulated with nigericin in the presence of the pan-caspase inhibitor ZVAD or the caspase-1 inhibitor YVAD at the indicated concentration (μM) and examined for IL-1β secretion after 2 h (D), intracellular K^+ (E), and LDH (F). Histograms are means ± SD of three samples per treatment condition and are representative of two similar experiments with neutrophils from different donors. $^{**}p < 0.005$, $^{***}p < 0.0005$.

on a global scale (35, 36). *S. pneumoniae* is also a leading cause of corneal ulcers worldwide, resulting in visual impairment and blindness, especially in developing countries where the organisms are resident in the conjunctiva and enter the corneal stroma following an abrasion (37–39). In a study of individuals with *S. pneumoniae* corneal ulcers, neutrophils comprised >90% of the total cells; furthermore, expression of IL-1β, NLRP3, and ASC in corneal ulcers was greatly elevated compared with normal corneas (23).

Neutrophils are a source of proinflammatory and regulatory cytokines, including IFN-γ and IL-17A (19, 40, 41). Furthermore, although neutrophils are generally considered to be short-lived cells in the circulation, other reports indicate that these cells can survive for longer periods of time under inflammatory conditions where they are stimulated by proinflammatory cytokines and growth factors (42).

NLRP3 inflammasome activation and IL-1β processing have been extensively studied in monocytes, macrophages, and dendritic cells (3, 24); however, although neutrophils are the most prominent cells infiltrating sites in the early stages of infection and inflammation, the contribution of neutrophils to inflammasome activation and IL-1β production is less well understood.

Neutrophils are a major source of IL-1β in murine models of arthritis and osteomyelitis; however, as with our study on *P. aeruginosa* keratitis, IL-1β processing was caspase-1–independent and occurred as a result of cleavage by neutrophil proteases (5, 6, 43). In contrast, proteases and caspase-1 both contributed to IL-1β processing by LPS plus ATP–stimulated human neutrophils (44). However, our present findings are in agreement with a report showing that neutrophils are a major source of IL-1β in a *Staphylococcus aureus* model of skin abscess formation; furthermore, these investigators showed that *S. aureus*–induced IL-1β secretion by bone marrow neutrophils was impaired in ASC$^{-/-}$ mice and in the presence of NLRP3 and caspase-1 inhibitors, thereby implicating the NLRP3 inflammasome (45). Further, IL-1β secretion by murine bone marrow neutrophils stimulated with nigericin was dependent on expression of NLRP3 and ASC (46). We also show that the NLRP3 inflammasome is required for IL-1β cleavage during *S. pneumoniae* corneal infection, and we demonstrate that neutrophils recruited to infected corneas have active caspase-1 as detected by YVAD-FLICA.

In the present study, we have shown the results of multiple, highly reproducible experiments demonstrating that neutrophils form NLRP3/ASC/caspase 1 oligomers that are detected as multiple specks, including: 1) the presence of caspase-1 (using FLICA-YVAD) specks in neutrophils isolated from infected corneas; 2) the presence of multiple NLRP3 specks in bone marrow neutrophils following signal 1 and signal 2, as shown in Supplemental Videos 1 and 2; 3) the presence of ASC monomers in neutrophils given signal 1, and ASC multimeric complexes following signal 2; and 4) quantification of ASC and caspase-1 specks in isolated neutrophils given signals 1 and 2.

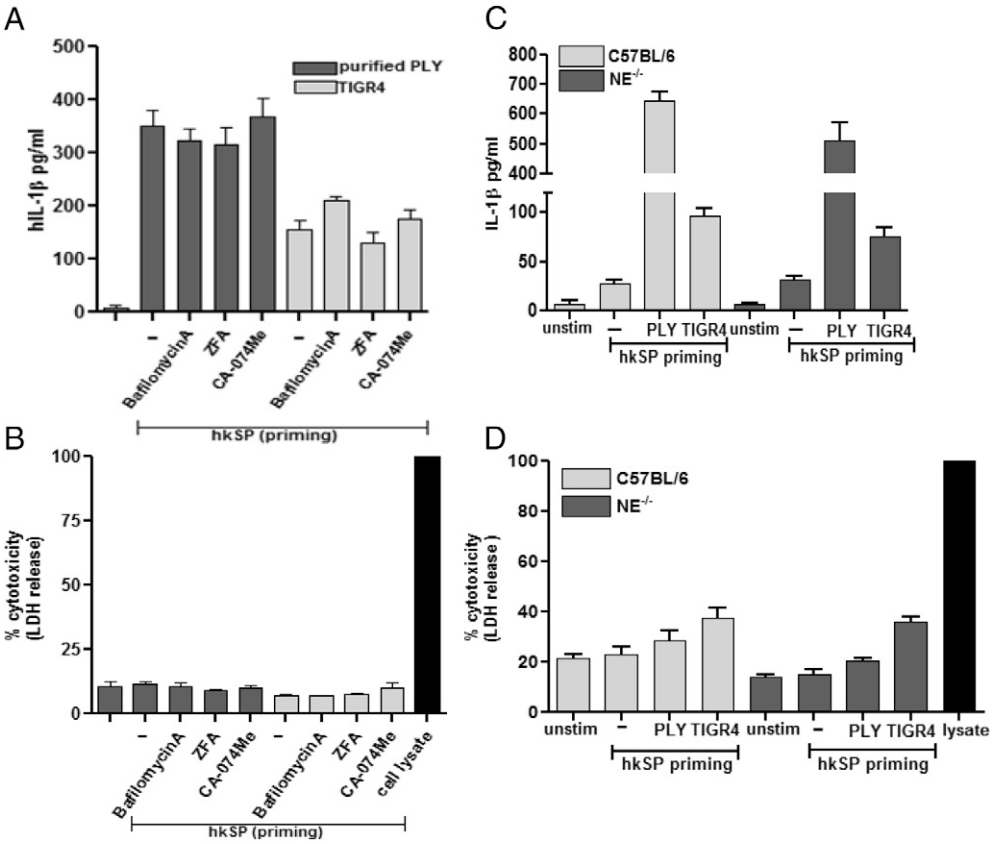

FIGURE 8. Ply-induced IL-1β secretion by neutrophils does not require lysosomal disruption or serine protease activity. (**A** and **B**) Primed human neutrophils were pretreated with bafilomycin A (200 nM), CA-074-Me (100 μM), or ZFA (50 μM) 30 min prior to stimulation with TIGR4 (50:1) or Ply (500 ng/ml) for 2 h, and IL-1β (A) and LDH (B) release were quantified from the supernatant. (**C** and **D**) Primed murine neutrophils from C57BL/6 and $NE^{-/-}$ mice were stimulated with TIGR4 (50:1) or Ply (500 ng/ml) for 2 h, and IL-1β (C) and LDH (D) release were quantified. Histograms are means ± SD of samples of five samples per treatment condition and are representative of three independent experiments with similar observations.

The presence of multiple specks in neutrophils is clearly distinct from dendritic cells and macrophages, which mostly show a single speck per cell (3), although multiple specks were detected in macrophages from patients with a gain-of-function mutation in NLRC4 (47). The significance of multiple versus single inflammasome oligomers in neutrophils has yet to be determined; however, it is very clear that neutrophils are a major source of mature IL-1β, at least at early stages of infection, and that activation of caspase-1 through the NLRP3/ASC inflammasome is essential for processing IL-1β.

We reported that neutrophils are an important source of IL-1β in *P. aeruginosa* corneal infection, and that cleavage is a result of serine protease activity and is independent of caspase-1 and the NLRC4 inflammasome (6). In contrast to that study, we now show that although neutrophils are a major source of IL-1β in *S. pneumoniae* keratitis, caspase-1 is required for IL-1β cleavage and is activated by the NLRP3/ASC inflammasome. The difference between these models has yet to be determined but may be due to relatively low NLRC4 expression by neutrophils compared with macrophages (46).

To characterize the mechanisms by which the NLRP3 inflammasome is activated in human neutrophils, we examined two pathways: 1) the channel mode that results in loss of cytosolic K^+, and 2) the cathepsin B pathway that is activated by lysosome rupture following phagocytosis (48). We also examined the role of pyroptosis in this process. Our data are consistent with the first pathway in which active Ply causes loss of intracellular K^+. Because caspase-1 inhibitors blocked IL-1β secretion, but did not inhibit K^+ efflux, we conclude that Ply-induced K^+ efflux occurs upstream and independently of caspase-1–mediated IL-1β processing and is not a secondary consequence of caspase-1–driven pyroptosis. This finding that NLRP3 activation in neutrophils does not lead to pyroptosis is in agreement with a recent study demonstrating that neutrophils do not undergo NLRC4-mediated pyroptotic cell death following stimulation with *Salmonella* (49). Although the molecular basis for the absence of pyroptosis in neutrophils compared with macrophages has yet to be defined, a possible advantage is that bacteria are released from dead macrophages and can then be killed by neutrophils (50). Furthermore, in contrast to macrophages, neutrophils undergo cell death where the nucleus decondenses and chromatin is released from the cell to form neutrophil extracellular traps, which also contain antimicrobial peptides and proteases that are effective in killing microbial pathogens (51, 52).

Lysosomal destabilization and cathepsin B activation contribute to *S. pneumoniae*–induced NLRP3 activation in monocytes and macrophages (31); however, we found no role for cathepsin B in neutrophil-mediated IL-1β processing, whereas our findings on the role of K^+ efflux are consistent with a recent study showing that K^+ efflux is critical for activation of the NLRP3 inflammasome in bone marrow macrophages and dendritic cells (14, 27). Although activated in response to structurally distinct agents including silica, asbestos, uric acid crystals, and bacterial toxins, as well as damage-associated molecular patterns including ATP, a common response to all NLRP3-activating stimuli is a change in plasma membrane permeability that leads to efflux of intracellular potassium. Ply has been shown to induce K^+ efflux in macrophages (35, 53), and we now show that this is also required in human neutrophils.

Ply is an important virulence factor in *S. pneumoniae* infections, and it is expressed in clinical isolates from *S. pneumoniae* infections, including corneal ulcers (23, 35). Ply is a cholesterol-dependent cytolysin that forms oligomers in the host cell plasma membrane (~40 monomers), resulting in formation of large (~400 Å) transmembrane pores that cause rapid cell lysis (54). Although reported as a cytoplasmic protein that is released after autolysis (35), Ply was more recently shown to localize in the bacterial cell wall where it is released following cleavage by extracellular proteases (55, 56). Ply activates the NLRP3 inflammasome in monocytes, macrophages, and dendritic cells in pneumococcal pneumonia (14, 57), and Ply-expressing *S. pneumoniae* strains induce keratitis in animal models (58, 59). In the present study, we demonstrated that NLRP3 oligomerization, caspase-1 activation, and IL-1β processing in human and murine neutrophils are dependent on expression of the hemolytic activity of Ply, as neither the *S. pneumoniae* Δ*ply* mutant nor the nonhemolytic PdB toxoid induced this response. Similarly, *S. aureus*–induced IL-1β secretion by neutrophils required expression of the pore-forming α-toxin (45).

Oligomerization of the NLRP3/ASC inflammasome can be visualized as discrete intracellular specks in macrophages and dendritic cells (3); however, we demonstrate that caspase-1 specks are generated in activated neutrophils in vitro and in vivo following *S. pneumoniae* corneal infection. We also show that ASC forms multimeric complexes in Ply-activated neutrophils, which is similar to that described in macrophages (3, 27). However, in contrast to macrophages that have single specks (3), we consistently found that stimulated murine and human neutrophils have multiple specks. The basis for this difference has yet to be determined.

We used caspase-$1^{-/-}$ mice that are also deficient in caspase-11 activity; however, we show specific caspase-1 activity by neutrophils using FLICA-YVAD, and we block IL-1β production by neutrophils using the specific caspase-1 inhibitor YVAD. Taken together, these findings support a role for caspase-1 rather than caspase-11 in this process.

The results of the present study add to our understanding of the role of neutrophil-derived IL-1β in bacterial infections by demonstrating that neutrophils are not only an important source of this cytokine during bacterial infection, but also form NLRP3/ASC inflammasome aggregates in vivo that activate caspase-1 and mediate IL-1β cleavage and secretion. Furthermore, although we show that requirement for K^+ efflux in Ply-induced NLRP3 activation in neutrophils is similar to macrophages (14, 57), there are distinct differences between these cell types, including susceptibility to pyroptosis.

In conclusion, given the diverse infectious and inflammatory conditions where neutrophils infiltrate the tissues in large numbers, it seems highly likely that their role in IL-1β–mediated inflammation will be found in multiple diseases.

Disclosures

The authors have no financial conflicts of interest.

References

1. Dinarello, C. A. 2009. Immunological and inflammatory functions of the interleukin-1 family. *Annu. Rev. Immunol.* 27: 519–550.
2. Dinarello, C. A., A. Simon, and J. W. van der Meer. 2012. Treating inflammation by blocking interleukin-1 in a broad spectrum of diseases. *Nat. Rev. Drug Discov.* 11: 633–652.
3. Latz, E., T. S. Xiao, and A. Stutz. 2013. Activation and regulation of the inflammasomes. *Nat. Rev. Immunol.* 13: 397–411.
4. Gross, O., C. J. Thomas, G. Guarda, and J. Tschopp. 2011. The inflammasome: an integrated view. *Immunol. Rev.* 243: 136–151.
5. Guma, M., L. Ronacher, R. Liu-Bryan, S. Takai, M. Karin, and M. Corr. 2009. Caspase 1-independent activation of interleukin-1β in neutrophil-predominant inflammation. *Arthritis Rheum.* 60: 3642–3650.
6. Karmakar, M., Y. Sun, A. G. Hise, A. Rietsch, and E. Pearlman. 2012. Cutting edge: IL-1β processing during *Pseudomonas aeruginosa* infection is mediated by neutrophil serine proteases and is independent of NLRC4 and caspase-1. *J. Immunol.* 189: 4231–4235.
7. Joosten, L. A., M. G. Netea, G. Fantuzzi, M. I. Koenders, M. M. Helsen, H. Sparrer, C. T. Pham, J. W. van der Meer, C. A. Dinarello, and W. B. van den Berg. 2009. Inflammatory arthritis in caspase 1 gene-deficient mice: contribution of proteinase 3 to caspase 1-independent production of bioactive interleukin-1β. *Arthritis Rheum.* 60: 3651–3662.
8. Lamkanfi, M., and V. M. Dixit. 2014. Mechanisms and functions of inflammasomes. *Cell* 157: 1013–1022.
9. Kuida, K., J. A. Lippke, G. Ku, M. W. Harding, D. J. Livingston, M. S. Su, and R. A. Flavell. 1995. Altered cytokine export and apoptosis in mice deficient in interleukin-1 beta converting enzyme. *Science* 267: 2000–2003.
10. Broz, P., T. Ruby, K. Belhocine, D. M. Bouley, N. Kayagaki, V. M. Dixit, and D. M. Monack. 2012. Caspase-11 increases susceptibility to *Salmonella* infection in the absence of caspase-1. *Nature* 490: 288–291.
11. Kanneganti, T. D., N. Ozören, M. Body-Malapel, A. Amer, J. H. Park, L. Franchi, J. Whitfield, W. Barchet, M. Colonna, P. Vandenabeele, et al. 2006. Bacterial RNA and small antiviral compounds activate caspase-1 through cryopyrin/Nalp3. *Nature* 440: 233–236.
12. Sun, Y., M. Karmakar, S. Roy, R. T. Ramadan, S. R. Williams, S. Howell, C. L. Shive, Y. Han, C. M. Stopford, A. Rietsch, and E. Pearlman. 2010. TLR4 and TLR5 on corneal macrophages regulate *Pseudomonas aeruginosa* keratitis by signaling through MyD88-dependent and -independent pathways. *J. Immunol.* 185: 4272–4283.
13. Gilbert, R. J., J. Rossjohn, M. W. Parker, R. K. Tweten, P. J. Morgan, T. J. Mitchell, N. Errington, A. J. Rowe, P. W. Andrew, and O. Byron. 1998. Self-interaction of pneumolysin, the pore-forming protein toxin of *Streptococcus pneumoniae*. *J. Mol. Biol.* 284: 1223–1237.
14. McNeela, E. A., A. Burke, D. R. Neill, C. Baxter, V. E. Fernandes, D. Ferreira, S. Smeaton, R. El-Rachkidy, R. M. McLoughlin, A. Mori, et al. 2010. Pneumolysin activates the NLRP3 inflammasome and promotes proinflammatory cytokines independently of TLR4. *PLoS Pathog.* 6: e1001191.
15. Franzen, C. A., P. E. Simms, A. F. Van Huis, K. E. Foreman, P. C. Kuo, and G. N. Gupta. 2014. Characterization of uptake and internalization of exosomes by bladder cancer cells. *Biomed Res. Int.* 2014: 619829.
16. Kahlenberg, J. M., and G. R. Dubyak. 2004. Mechanisms of caspase-1 activation by P2X7 receptor-mediated K^+ release. *Am. J. Physiol. Cell Physiol.* 286: C1100–C1108.
17. Hamrah, P., Y. Liu, Q. Zhang, and M. R. Dana. 2003. The corneal stroma is endowed with a significant number of resident dendritic cells. *Invest. Ophthalmol. Vis. Sci.* 44: 581–589.
18. Knickelbein, J. E., S. C. Watkins, P. G. McMenamin, and R. L. Hendricks. 2009. Stratification of antigen-presenting cells within the normal cornea. *Ophthalmol Eye Dis* 1: 45–54.
19. Taylor, P. R., S. Roy, S. M. Leal, Jr., Y. Sun, S. J. Howell, B. A. Cobb, X. Li, and E. Pearlman. 2014. Activation of neutrophils by autocrine IL-17A–IL-17RC interactions during fungal infection is regulated by IL-6, IL-23, RORγt and dectin-2. *Nat. Immunol.* 15: 143–151.
20. Meissner, F., R. A. Seger, D. Moshous, A. Fischer, J. Reichenbach, and A. Zychlinsky. 2010. Inflammasome activation in NADPH oxidase defective mononuclear phagocytes from patients with chronic granulomatous disease. *Blood* 116: 1570–1573.
21. Sokolovska, A., C. E. Becker, W. K. Ip, V. A. Rathinam, M. Brudner, N. Paquette, A. Tanne, S. K. Vanaja, K. J. Moore, K. A. Fitzgerald, et al. 2013. Activation of caspase-1 by the NLRP3 inflammasome regulates the NADPH oxidase NOX2 to control phagosome function. *Nat. Immunol.* 14: 543–553.
22. Tullos, N. A., H. W. Thompson, S. D. Taylor, M. Sanders, E. W. Norcross, I. Tolo, Q. Moore, and M. E. Marquart. 2013. Modulation of immune signaling, bacterial clearance, and corneal integrity by Toll-like receptors during *Streptococcus pneumoniae* keratitis. *Curr. Eye Res.* 38: 1036–1048.
23. Karthikeyan, R. S., J. L. Priya, S. M. Leal, Jr., J. Toska, A. Rietsch, V. Prajna, E. Pearlman, and P. Lalitha. 2013. Host response and bacterial virulence factor expression in *Pseudomonas aeruginosa* and *Streptococcus pneumoniae* corneal ulcers. *PLoS ONE* 8: e64867.
24. Franchi, L., R. Muñoz-Planillo, and G. Núñez. 2012. Sensing and reacting to microbes through the inflammasomes. *Nat. Immunol.* 13: 325–332.
25. Ataide, M. A., W. A. Andrade, D. S. Zamboni, D. Wang, Mdo. C. Souza, B. S. Franklin, S. Elian, F. S. Martins, D. Pereira, G. Reed, et al. 2014. Malaria-induced NLRP12/NLRP3-dependent caspase-1 activation mediates inflammation and hypersensitivity to bacterial superinfection. *PLoS Pathog.* 10: e1003885.
26. Subramanian, N., K. Natarajan, M. R. Clatworthy, Z. Wang, and R. N. Germain. 2013. The adaptor MAVS promotes NLRP3 mitochondrial localization and inflammasome activation. *Cell* 153: 348–361.
27. Muñoz-Planillo, R., P. Kuffa, G. Martínez-Colón, B. L. Smith, T. M. Rajendiran, and G. Núñez. 2013. K^+ efflux is the common trigger of NLRP3 inflammasome activation by bacterial toxins and particulate matter. *Immunity* 38: 1142–1153.
28. Sagulenko, V., S. J. Thygesen, D. P. Sester, A. Idris, J. A. Cridland, P. R. Vajjhala, T. L. Roberts, K. Schroder, J. E. Vince, J. M. Hill, et al. 2013. AIM2 and NLRP3 inflammasomes activate both apoptotic and pyroptotic death pathways via ASC. *Cell Death Differ.* 20: 1149–1160.
29. Fernandes-Alnemri, T., J. Wu, J. W. Yu, P. Datta, B. Miller, W. Jankowski, S. Rosenberg, J. Zhang, and E. S. Alnemri. 2007. The pyroptosome: a supra-

molecular assembly of ASC dimers mediating inflammatory cell death via caspase-1 activation. *Cell Death Differ.* 14: 1590–1604.
30. Hornung, V., F. Bauernfeind, A. Halle, E. O. Samstad, H. Kono, K. L. Rock, K. A. Fitzgerald, and E. Latz. 2008. Silica crystals and aluminum salts activate the NALP3 inflammasome through phagosomal destabilization. *Nat. Immunol.* 9: 847–856.
31. Hoegen, T., N. Tremel, M. Klein, B. Angele, H. Wagner, C. Kirschning, H. W. Pfister, A. Fontana, S. Hammerschmidt, and U. Koedel. 2011. The NLRP3 inflammasome contributes to brain injury in pneumococcal meningitis and is activated through ATP-dependent lysosomal cathepsin B release. *J. Immunol.* 187: 5440–5451.
32. Stehlik, C. 2009. Multiple interleukin-1β-converting enzymes contribute to inflammatory arthritis. *Arthritis Rheum.* 60: 3524–3530.
33. Black, R. A., S. R. Kronheim, M. Cantrell, M. C. Deeley, C. J. March, K. S. Prickett, J. Wignall, P. J. Conlon, D. Cosman, T. P. Hopp, et al. 1988. Generation of biologically active interleukin-1 beta by proteolytic cleavage of the inactive precursor. *J. Biol. Chem.* 263: 9437–9442.
34. Hazuda, D. J., J. Strickler, F. Kueppers, P. L. Simon, and P. R. Young. 1990. Processing of precursor interleukin 1 beta and inflammatory disease. *J. Biol. Chem.* 265: 6318–6322.
35. Kadioglu, A., J. N. Weiser, J. C. Paton, and P. W. Andrew. 2008. The role of *Streptococcus pneumoniae* virulence factors in host respiratory colonization and disease. *Nat. Rev. Microbiol.* 6: 288–301.
36. Denny, F. W., and F. A. Loda. 1986. Acute respiratory infections are the leading cause of death in children in developing countries. *Am. J. Trop. Med. Hyg.* 35: 1–2.
37. Bharathi, M. J., R. Ramakrishnan, R. Meenakshi, S. Padmavathy, C. Shivakumar, and M. Srinivasan. 2007. Microbial keratitis in South India: influence of risk factors, climate, and geographical variation. *Ophthalmic Epidemiol.* 14: 61–69.
38. Parmar, P., A. Salman, C. M. Kalavathy, C. A. Jesudasan, and P. A. Thomas. 2003. Pneumococcal keratitis: a clinical profile. *Clin. Experiment. Ophthalmol.* 31: 44–47.
39. Upadhyay, M. P., P. C. Karmacharya, S. Koirala, N. R. Tuladhar, L. E. Bryan, G. Smolin, and J. P. Whitcher. 1991. Epidemiologic characteristics, predisposing factors, and etiologic diagnosis of corneal ulceration in Nepal. *Am. J. Ophthalmol.* 111: 92–99.
40. Mantovani, A., M. A. Cassatella, C. Costantini, and S. Jaillon. 2011. Neutrophils in the activation and regulation of innate and adaptive immunity. *Nat. Rev. Immunol.* 11: 519–531.
41. Sturge, C. R., A. Benson, M. Raetz, C. L. Wilhelm, J. Mirpuri, E. S. Vitetta, and F. Yarovinsky. 2013. TLR-independent neutrophil-derived IFN-γ is important for host resistance to intracellular pathogens. *Proc. Natl. Acad. Sci. USA* 110: 10711–10716.
42. Kolaczkowska, E., and P. Kubes. 2013. Neutrophil recruitment and function in health and inflammation. *Nat. Rev. Immunol.* 13: 159–175.
43. Cassel, S. L., J. R. Janczy, X. Bing, S. P. Wilson, A. K. Olivier, J. E. Otero, Y. Iwakura, D. M. Shayakhmetov, A. G. Bassuk, Y. Abu-Amer, et al. 2014. Inflammasome-independent IL-1β mediates autoinflammatory disease in Pstpip2-deficient mice. *Proc. Natl. Acad. Sci. USA* 111: 1072–1077.
44. Gabelloni, M. L., F. Sabbione, C. Jancic, J. Fuxman Bass, I. Keitelman, L. Iula, M. Oleastro, J. R. Geffner, and A. S. Trevani. 2013. NADPH oxidase derived reactive oxygen species are involved in human neutrophil IL-1β secretion but not in inflammasome activation. *Eur. J. Immunol.* 43: 3324–3335.
45. Cho, J. S., Y. Guo, R. I. Ramos, F. Hebroni, S. B. Plaisier, C. Xuan, J. L. Granick, H. Matsushima, A. Takashima, Y. Iwakura, et al. 2012. Neutrophil-derived IL-1β is sufficient for abscess formation in immunity against *Staphylococcus aureus* in mice. *PLoS Pathog.* 8: e1003047.
46. Mankan, A. K., T. Dau, D. Jenne, and V. Hornung. 2012. The NLRP3/ASC/caspase-1 axis regulates IL-1β processing in neutrophils. *Eur. J. Immunol.* 42: 710–715.
47. Romberg, N., K. Al Moussawi, C. Nelson-Williams, A. L. Stiegler, E. Loring, M. Choi, J. Overton, E. Meffre, M. K. Khokha, A. J. Huttner, et al. 2014. Mutation of NLRC4 causes a syndrome of enterocolitis and autoinflammation. *Nat. Genet.* 46: 1135–1139.
48. Tschopp, J., and K. Schroder. 2010. NLRP3 inflammasome activation: the convergence of multiple signalling pathways on ROS production? *Nat. Rev. Immunol.* 10: 210–215.
49. Chen, K. W., C. J. Groß, F. V. Sotomayor, K. J. Stacey, J. Tschopp, M. J. Sweet, and K. Schroder. 2014. The neutrophil NLRC4 inflammasome selectively promotes IL-1β maturation without pyroptosis during acute *Salmonella* challenge. *Cell Reports* 8: 570–582.
50. Miao, E. A., I. A. Leaf, P. M. Treuting, D. P. Mao, M. Dors, A. Sarkar, S. E. Warren, M. D. Wewers, and A. Aderem. 2010. Caspase-1-induced pyroptosis is an innate immune effector mechanism against intracellular bacteria. *Nat. Immunol.* 11: 1136–1142.
51. Brinkmann, V., U. Reichard, C. Goosmann, B. Fauler, Y. Uhlemann, D. S. Weiss, Y. Weinrauch, and A. Zychlinsky. 2004. Neutrophil extracellular traps kill bacteria. *Science* 303: 1532–1535.
52. Kaplan, M. J., and M. Radic. 2012. Neutrophil extracellular traps: double-edged swords of innate immunity. *J. Immunol.* 189: 2689–2695.
53. Franchi, L., T. D. Kanneganti, G. R. Dubyak, and G. Núñez. 2007. Differential requirement of P2X7 receptor and intracellular K^+ for caspase-1 activation induced by intracellular and extracellular bacteria. *J. Biol. Chem.* 282: 18810–18818.
54. Tilley, S. J., E. V. Orlova, R. J. Gilbert, P. W. Andrew, and H. R. Saibil. 2005. Structural basis of pore formation by the bacterial toxin pneumolysin. *Cell* 121: 247–256.
55. Price, K. E., and A. Camilli. 2009. Pneumolysin localizes to the cell wall of *Streptococcus pneumoniae*. *J. Bacteriol.* 191: 2163–2168.
56. Price, K. E., N. G. Greene, and A. Camilli. 2012. Export requirements of pneumolysin in *Streptococcus pneumoniae*. *J. Bacteriol.* 194: 3651–3660.
57. Witzenrath, M., F. Pache, D. Lorenz, U. Koppe, B. Gutbier, C. Tabeling, K. Reppe, K. Meixenberger, A. Dorhoi, J. Ma, et al. 2011. The NLRP3 inflammasome is differentially activated by pneumolysin variants and contributes to host defense in pneumococcal pneumonia. *J. Immunol.* 187: 434–440.
58. Moore, Q. C., III, C. C. McCormick, E. W. Norcross, C. Onwubiko, M. E. Sanders, J. Fratkin, L. S. McDaniel, R. J. O'Callaghan, and M. E. Marquart. 2009. Development of a *Streptococcus pneumoniae* keratitis model in mice. *Ophthalmic Res.* 42: 141–146.
59. Reed, J. M., R. J. O'Callaghan, D. O. Girgis, C. C. McCormick, A. R. Caballero, and M. E. Marquart. 2005. Ocular virulence of capsule-deficient *streptococcus pneumoniae* in a rabbit keratitis model. *Invest. Ophthalmol. Vis. Sci.* 46: 604–608.